



The key role of hydrogen bonding in the nuclearity of three copper(II) complexes with hydrazone-derived ligands and nitrogen donor heterocycles

Shyamapada Shit^a, Subrata K. Dey^b, Corrado Rizzoli^c, Ennio Zangrando^d, Guillaume Pilet^e, Carlos J. Gómez-García^f, Samiran Mitra^{a,*}

^a Department of Chemistry, Jadavpur University, Kolkata 700 032, West Bengal, India

^b Department of Chemistry, Bankura Sammilani College, Kenduadihi, Bankura 722 102, West Bengal, India

^c Università degli Studi di Parma, Dip. di Chimica GIAF, Viale G.P. Usberti 17/A, I-43100 Parma, Italy

^d Università degli Studi di Trieste, Dip. di Scienze Chimiche e Farmaceutiche, Via Licio Giorgieri, 1, 34127 Trieste, Italy

^e Groupe de Cristallographie et Ingénierie Moléculaire, Laboratoire des Multimatériaux et Interfaces, UMR 5615, Université Claude Bernard Lyon 1, Bât. Jules Roulin, 43 Bd du 11 Novembre, 1918-69622 Villeurbanne Cedex, France

^f Instituto de Ciencia Molecular, ICMol, Universidad de Valencia, Parque Científico, 46980 Paterna, Spain

ARTICLE INFO

Article history:

Received 10 May 2010

Received in revised form 28 November 2010

Accepted 8 January 2011

Available online 19 January 2011

Keywords:

Cu(II) hydrazone complexes

Crystal structures

Monodentate pyz and 4,4'-bpy

Self assembly

Hydrogen bonding

Antiferromagnetic coupling

ABSTRACT

Three new Cu(II) complexes of formula $[\text{Cu}(\text{L}^1)(\text{pyz})(\text{CH}_3\text{OH})]\text{ClO}_4$ (**1**), $[\text{Cu}(\text{L}^1)(4,4'\text{-bpy})(\text{ClO}_4)] \cdot 0.5\text{H}_2\text{O}$ (**2**) and $[\{\text{Cu}(\text{L}^2)(\text{ClO}_4)\}_2(\mu\text{-}4,4'\text{-bpy})]$ (**3**) have been synthesised by using pyrazine (pyz) and 4,4'-bipyridine (4,4'-bpy) and tridentate O,N,O-donor hydrazone ligands, L¹H and L²H, obtained by the condensation of 1,1,1-trifluoro-2,4-pentanedione with salicyloylhydrazide and benzhydrazide, respectively. The ligands and their complexes have been characterized by elemental analyses, FT-IR, and UV–Vis spectroscopies. Single crystal X-ray structure analysis evidences the metal ion in a slightly deformed square pyramidal geometry in all the complexes. However complexes **1** and **2** are mononuclear with pyz and 4,4'-bpy, respectively, showing an unusual monodentate behavior, while complex **3** is dinuclear with 4,4'-bpy adopting the typical bridging coordination mode. Self assembly of the complex units by hydrogen bonding interactions produces one-dimensional arrangement in each crystal packing. The magnetic characterization of complex **3** indicates a weak antiferromagnetic exchange interaction between the Cu(II) ions ($J = -0.96 \text{ cm}^{-1}$) mediated through the long 4,4'-bpy bridge. Electrochemical behavior of the complexes is also discussed.

© 2011 Elsevier B.V. All rights reserved.

1. Introduction

The self-assembly of molecular building blocks containing organic ligand and transition metal ions provides a reliable and efficient approach for the design and construction of metal-organic frameworks (MOFs). The interest in this field is due to the potential use of the compounds as metal-based molecules, host guest properties, magnetic materials, etc. [1]. Among the various organic ligands, Schiff bases have become an obvious choice not only for their synthetic flexibility, structural variety and varied denticity [2], but also for their selectivity as well as sensitivity towards transition metal ions. In this regard, hydrazones have got special importance due to their chemical as well as biological applications [3]. Moreover, due to keto-enol tautomerism, they can provide neutral [4], mono- [5], di- [6–8], or tetraanionic [9] species leading to unusual coordination numbers [6,10]. Mono- or di-nuclear complexes are synthesized depending upon the reaction conditions

such as nature and concentration of the metal, pH of the medium and hydrazone ligand properties [5]. Aryl hydrazones are well known as a class of versatile ligands capable of forming different molecular architectures and coordination polymers. Their transition metal complexes show electrical and magnetic properties [11] and are used in synthetic and analytical chemistry as novel heterogeneous catalysts in oxido-reduction processes, various chemical and photochemical reactions [12,13], as well as in numerous industrial applications. Arylhydrazone metal complexes are also important for their possible biological applications [14,15–21]. In this regard, Cu(II) hydrazones can be mentioned for their structural richness, biological activities as well as for understanding the effects of structural and chemical factors that govern the exchange coupling between paramagnetic centers [22–31].

Self-assembly of molecular building blocks can also be achieved in a controlled manner through the use of bridging heterocyclic bidentate amine ligands such as 4,4'-bipyridine (4,4'-bpy), pyrazine (pyz) and their derivatives. Many examples are known where 4,4'-bpy and pyz act as a linear rigid spacer between metal centers to form coordination polymers of different dimensionalities [32].

* Corresponding author. Tel.: +91 33 2414 6666x2505; fax: +91 33 2414 6414.
E-mail address: smitra_2002@yahoo.com (S. Mitra).

Moreover, hydrogen bonding has been applied in self-assembly of molecular building blocks containing appropriate groups with the aim of generating discrete or extensive supramolecular entities. Sometimes self assembly through hydrogen bonding interaction acts as a structure directing force and formation of higher dimensionality structures are hindered regardless of the presence of such bridging ligands [33–35].

In this paper, we describe the synthesis, spectral and structural characterization of three new Cu(II) complexes of formulation $[\text{Cu}(\text{L}^1)(\text{pyz})(\text{CH}_3\text{OH})]\text{ClO}_4$ (**1**), $[\text{Cu}(\text{L}^1)(4,4'\text{-bpy})(\text{ClO}_4)] \cdot 0.5\text{H}_2\text{O}$ (**2**), and $[\{\text{Cu}(\text{L}^2)(\text{ClO}_4)\}_2(\mu\text{-}4,4'\text{-bpy})]$ (**3**), derived from two different O,N,O-donor tridentate hydrazone ligands L^1H and L^2H (Scheme 1), and N-donor heterocycles such as pyrazine (pyz), and 4,4'-bipyridine (4,4'-bpy). We have also explored the conjugate effect of 4,4'-bpy and pyz and the hydrogen bonding interaction on the self-assembly process of the building blocks. The magnetic properties of the three compounds are also reported. In complex **3** the thermal variation of the magnetic susceptibility shows the presence of a weak antiferromagnetic exchange interaction that has been satisfactorily reproduced with a simple $S = 1/2$ dimer model with $J = -0.96(1) \text{ cm}^{-1}$.

2. Experimental

2.1. Materials

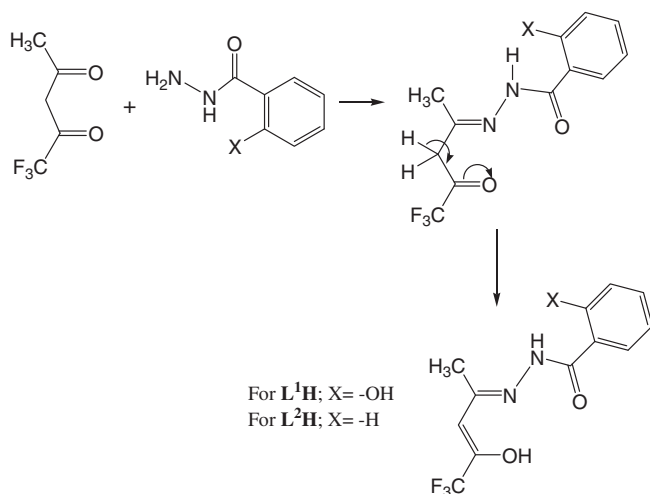
1,1,1-Trifluoro-2,4-pentanedione, salicyloylhydrazide, benzhydrazone, pyrazine, 4,4'-bipyridine, and $\text{Cu}(\text{ClO}_4)_2 \cdot 6\text{H}_2\text{O}$ were purchased from Aldrich Chemical Co. and used without further purification. All other chemicals and solvents were of analytical reagent grade and used as received.

2.2. Syntheses of the ligands and complexes

Caution! Perchlorate salts of transition metal ions in presence of organic ligands are potentially explosive, though no problems have been encountered during the syntheses of the complexes, they should be prepared in small quantities and handled with much care.

2.2.1. Syntheses of the Schiff base ligands (L^1H and L^2H)

2.2.1.1. $[\text{CF}_3\text{C}(\text{OH})=\text{CH}-\text{C}(\text{CH}_3)=\text{N}-\text{NH}-\text{CO}-\text{C}_6\text{H}_4(\text{OH})]$ (L^1H) and $[\text{CF}_3\text{C}(\text{OH})=\text{CH}-\text{C}(\text{CH}_3)=\text{N}-\text{NH}-\text{CO}-\text{C}_6\text{H}_5]$ (L^2H). The Schiff bases were prepared following a similar procedure by the reflux conden-



Scheme 1. Synthetic scheme of Schiff base ligands.

sation of 1,1,1-trifluoro-2,4-pentanedione (0.770 g, 5 mmol) with salicyloylhydrazide (0.760 g, 5 mmol) or benzhydrazone (0.680 g, 5 mmol) for L^1H and L^2H , respectively, in 100 mL of methanol for 2 h. The volume of the resultant yellow liquid was reduced to about 40 mL in a rotary evaporator. The crystalline ligands were obtained by slow evaporation of the mother liquor. L^1H , yield: 1.224 g (85%). *Anal. Calc.* for $\text{C}_{12}\text{H}_{11}\text{F}_3\text{N}_2\text{O}_3$: C, 50.01; H, 3.85; N, 9.72. Found: C, 50.01; H, 3.83; N, 9.70%. L^2H , yield: 1.20 g (88%). *Anal. Calc.* for $\text{C}_{12}\text{H}_{11}\text{F}_3\text{N}_2\text{O}_2$: C, 52.94; H, 4.07; N, 10.29. Found: C, 52.92; H, 4.05; N, 10.28%.

2.2.2. Syntheses of the complexes

2.2.2.1. $[\text{Cu}(\text{L}^1)(\text{pyz})(\text{CH}_3\text{OH})]\text{ClO}_4$ (**1**). A methanolic solution (20 mL) of the Schiff base L^1H (0.288 g, 1 mmol) was added to a methanolic solution (10 mL) of $\text{Cu}(\text{ClO}_4)_2 \cdot 6\text{H}_2\text{O}$ (0.371 g, 1 mmol) and stirred for 10 min. Then a 10 mL methanolic solution of pyrazine (0.80 g, 1 mmol) was added dropwise to the solution. The resulting solution was filtered and the filtrate kept undisturbed at room temperature for 4 days. Light green crystals suitable for X-ray diffraction quality were obtained after 4 days. Yield: 70% with respect to metal substrate. *Anal. Calc.* for $\text{C}_{17}\text{H}_{18}\text{CuF}_3\text{N}_4\text{O}_8\text{Cl}$: C, 36.31; H, 3.23; N, 9.96; Cu, 11.30. Found: C, 36.30; H, 3.21; N, 9.95; Cu, 11.29%.

2.2.2.2. $[\text{Cu}(\text{L}^1)(4,4'\text{-bpy})(\text{ClO}_4)] \cdot 0.5\text{H}_2\text{O}$ (**2**). To a methanolic solution (30 mL) of $\text{Cu}(\text{ClO}_4)_2 \cdot 6\text{H}_2\text{O}$ (0.371 g, 1 mmol) and L^1H (0.288 g, 1 mmol), a 20 mL methanolic solution of 4,4'-bipyridine (0.156 g, 1 mmol) was added dropwise with constant stirring. The solution was filtered and deep green single crystals of X-ray diffraction quality were obtained from the solution kept undisturbed at room temperature for 7 days. Yield: 74% with respect to metal substrate. *Anal. Calc.* for $\text{C}_{22}\text{H}_{19}\text{CuF}_3\text{N}_4\text{O}_{7.5}\text{Cl}$: C, 43.50; H, 3.15; N, 9.92; Cu, 10.33. Found: C, 43.47; H, 3.14; N, 9.91; Cu, 10.31%.

2.2.2.3. $[\{\text{Cu}(\text{L}^2)(\text{ClO}_4)\}_2(\mu\text{-}4,4'\text{-bpy})]$ (**3**). A methanolic solution (20 mL) of the Schiff base L^2H (0.272 g, 1 mmol) was added to a methanolic solution (10 mL) of $\text{Cu}(\text{ClO}_4)_2 \cdot 6\text{H}_2\text{O}$ (0.371 g, 1 mmol), and the resulting mixture was stirred for 30 min. Then a solution of 4,4'-bipyridine (0.062 g, 0.4 mmol) in 10 mL methanol was added dropwise. A white precipitate that appeared immediately was filtered and the filtrate was kept undisturbed for 7 days at room temperature from which deep green single crystals suitable for X-ray diffraction quality were obtained. Yield: 73% with respect to metal substrate. *Anal. Calc.* for $\text{C}_{34}\text{H}_{28}\text{Cl}_2\text{Cu}_2\text{F}_6\text{N}_6\text{O}_{12}$: C, 39.86; H, 2.75; N, 8.20; Cu, 12.40. Found: C, 39.85; H, 2.73; N, 8.18; Cu, 12.38%.

2.3. Physical measurements

Elemental analyses (carbon, hydrogen and nitrogen) were carried out with a Perkin–Elmer 2400 II elemental analyser. Copper content in the complexes have been estimated quantitatively by standard iodometric procedure. The FT-IR spectra ($4000\text{--}200 \text{ cm}^{-1}$) were recorded on a Perkin–Elmer Spectrum RX I FT-IR system with solid KBr pellets. The electronic spectra ($800\text{--}200 \text{ nm}$) were recorded on a Perkin–Elmer Lambda 40 UV-Vis spectrometer using HPLC grade acetonitrile as solvent. The concentrations of the solutions were $1 \times 10^{-5} \text{ M}$. Electrochemical studies were performed in acetonitrile on a VersaStat II cyclic voltammeter instrument and tetrabutylammonium perchlorate as the supporting electrolyte at a scan rate of 50 mV s^{-1} using platinum wire as working electrode and saturated calomel electrode (SCE) as reference. Variable temperature magnetic susceptibility measurements were carried out on polycrystalline samples with a Quantum Design MPMS-XL5 SQUID susceptometer, under an applied magnetic field of 0.1 T working in the temperature range of 2–300 K. The isothermal magnetization was performed on compound **3** at 2 K with

Table 1
Crystallographic data collection and structure refinement for **1**, **2** and **3**.

Parameters for	1	2	3
Empirical formula	C ₁₇ H ₁₈ CuF ₃ N ₄ O ₈ Cl	C ₂₂ H ₁₉ CuF ₃ N ₄ O _{7.5} Cl	C ₃₄ H ₂₈ Cl ₂ Cu ₂ F ₆ N ₆ O ₁₂
Formula weight	562.35	615.40	1024.61
Crystal system	triclinic	triclinic	orthorhombic
Space group	P $\bar{1}$ (No. 2)	P $\bar{1}$ (No. 2)	Fddd (No. 70)
<i>a</i> (Å)	8.328(2)	9.893(3)	20.2537(10)
<i>b</i> (Å)	11.056(3)	11.588(4)	25.8187(12)
<i>c</i> (Å)	12.662(3)	11.866(4)	30.1135(9)
α (°)	76.006(5)	105.05(3)	90.0
β (°)	89.407(6)	94.51(3)	90.0
γ (°)	76.211(5)	99.56(2)	90.0
<i>V</i> (Å ³)	1097.3(5)	1284.8(7)	15747.1(12)
<i>Z</i>	2	2	16
<i>T</i> (K)	295	293	293
<i>D</i> _{calc} (g cm ⁻³)	1.702	1.591	1.729
μ (mm ⁻¹)	1.195	1.027	1.315
<i>F</i> (0 0 0)	570	624	8256
θ Range for data collection (°)	1.7–25.3	2.9–25.3	1.4–27.9
Total data	11 366	15 834	15 850
<i>R</i> _{int}	0.049	0.035	0.047
Unique data	3963	4046	4706
Observed data [<i>I</i> > 2 σ (<i>I</i>)]	2309	2022	2329
Number parameters	307	359	280
Final <i>R</i> indices [<i>I</i> > 2 σ (<i>I</i>)] ^a	<i>R</i> ₁ = 0.0475, <i>wR</i> ₂ = 0.0658	<i>R</i> ₁ = 0.0566, <i>wR</i> ₂ = 0.1556	<i>R</i> ₁ = 0.0517, <i>wR</i> ₂ = 0.0568
<i>R</i> indices (all data) ^a	<i>R</i> ₁ = 0.0972, <i>wR</i> ₂ = 0.0697	<i>R</i> ₁ = 0.1030, <i>wR</i> ₂ = 0.1705	<i>R</i> ₁ = 0.0994, <i>wR</i> ₂ = 0.1018
Goodness-of-fit (GOF) on <i>F</i> ²	1.105	0.869	1.122
Residuals (e Å ⁻³)	0.35, -0.33	0.83, -0.29	0.96, -0.52

$$^a R = \sum(|F_o - F_c|) / \sum|F_o|, wR = \{\sum[w(|F_o - F_c|)^2] / \sum[w|F_o|^2]\}^{1/2}.$$

magnetic fields up to 8 T in a Quantum design PPMS9 equipment. Susceptibility data were corrected for the sample holder, previously measured under the same conditions, used for the diamagnetic contributions of complex **3**, as deduced by using Pascal's constant tables ($\chi_{\text{dia}} = -550.2 \text{ emu mol}^{-1}$).

2.4. X-ray crystallography

An air stable single crystal of **1** (of dimensions $0.18 \times 0.06 \times 0.05 \text{ mm}^3$), **2** ($0.15 \times 0.12 \times 0.08 \text{ mm}^3$) and **3** ($0.25 \times 0.26 \times 0.31 \text{ mm}^3$) were selected for diffraction data collections, which were performed at room temperature on a Bruker SMART 1000CCD, a Nonius DIP1030H system, and Nonius KappaCCD area diffractometer, respectively [36,37]. All the systems were equipped with graphite monochromated Mo K α radiation ($\lambda = 0.71073 \text{ \AA}$). Cell refinements and data reductions were carried out by using Bruker SAINT [38] for **1**, DENZO and SCALEPACK [39] for **2** and **3**. All the structures were solved by direct methods [40–42] combined to Fourier difference syntheses and refined with full-matrix least-squares based on *F*² with all observed reflections with all non-hydrogen atoms anisotropically treated. The contribution of hydrogen atoms at calculated positions were included in final cycles of refinements. A residual in ΔF map of **2** was interpreted as water oxygen (0.5 factor occupancy, H atoms not included). The molecular graphics and crystallographic illustrations were prepared using the ORTEP [43], and CAMERON program contained in the WinGX system [44]. Relevant crystallographic data and structure refinement parameters for the three complexes are summarized in Table 1.

3. Results and discussion

3.1. Description of molecular structures

For the syntheses of metal complexes two different hydrazone ligands (L¹H and L²H) have been employed. Reaction of L¹H and

Cu(ClO₄)₂·6H₂O with pyz or 4,4'-bpy in 1:1:1 ratio resulted in mononuclear complexes **1** and **2**, respectively, while the dinuclear complex **3** was obtained on reaction of L²H and Cu(ClO₄)₂·6H₂O with 4,4'-bpy in 1:1:0.4 ratio. Taking into account the structural results, we have performed a similar reaction of L²H and Cu(ClO₄)₂·6H₂O with pyz varying their stoichiometric ratios, but any attempt to get single crystals was unsuccessful.

An ORTEP view of complexes **1**, **2** and **3** with atom numbering scheme is shown in Figs. 1–3, respectively, and relevant bond lengths and angles are summarized in Table 2. X-ray crystallographic analyses reveal that compounds **1** and **2** consist of mononuclear complexes of formula [Cu(L¹)(pyz)(CH₃OH)]·ClO₄ and [Cu(L¹)(4,4'-bpy)(ClO₄)]·0.5H₂O, respectively, where pyz and 4,4'-bpy ligands coordinate the metal in the less usual monodentate fashion [45–50] in spite of their bridging behavior through the equivalent nitrogen donors. In fact, a survey of the CCDC database shows that of ca. 150 structures presenting Cu(II) ions and pyrazine, this ligand acts as monodentate only in eight cases, being a bridge in the remaining structures. Furthermore, of these eight structures only in four cases the copper complex is a monomer, as for compound **1**. Similarly the CCDC database was searched for structures comprising the 4,4'-bpy ligand and Cu(II) ions. Of ca. 450 structures retrieved, the 4,4'-bpy acts as a monodentate ligand only in 30 cases, being a bridge in the remaining structures. Of these 30 structures only in eight cases the copper complex is a monomer, as for compound **2**.

On the other hand, **3** is a dinuclear species {[Cu(L²)(ClO₄)]₂(μ -4,4'-bpy)}, where the 4,4'-bipyridine ligand, located on a crystallographic two-fold axis, connects the symmetry related [Cu(L²)(ClO₄)] units and spaces the metals by 10.968 Å.

Since most of the structural features are close comparable in **1**, **2**, and **3**, we describe first the coordination sphere, and then we will illustrate some differences in each structure and in the crystal packing. In all the complexes the metal ion has a slightly deformed square pyramid coordination sphere with a N₂O₃ chromophore satisfied by the hydrazone ligand and the heterocyclic organic N donor located in the basal plane, while an oxygen atom from

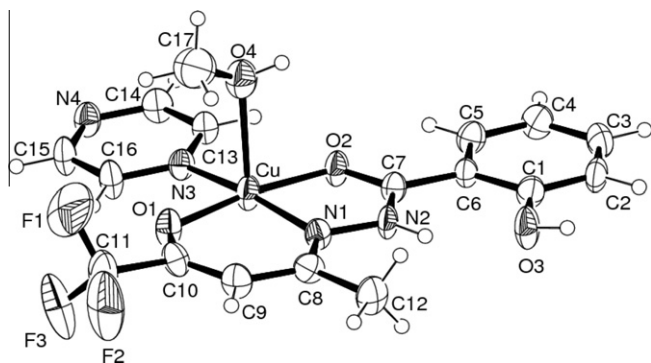


Fig. 1. ORTEP view of the complex cation of **1** with atom numbering scheme (thermal displacement ellipsoids are drawn at the 40% probability level).

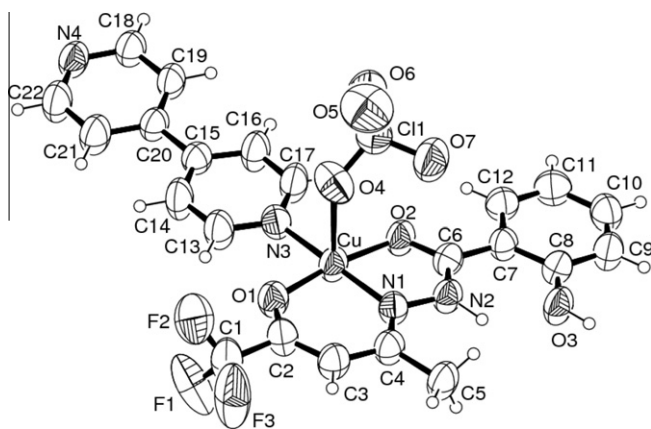


Fig. 2. ORTEP view of **2** with atom numbering scheme (thermal displacement ellipsoids are drawn at 40% probability level).

Table 2
Selected bond lengths (Å) and angles (°) for **1**, **2**, and **3**.

	1	2	3
Cu–O(1)	1.911(3)	1.897(4)	1.901(4)
Cu–O(2)	1.977(3)	1.969(4)	1.973(4)
Cu–N(1)	1.940(3)	1.929(4)	1.930(4)
Cu–N(3)	2.020(4)	1.984(5)	1.965(4)
Cu–O(4)	2.320(3)	2.449(5)	2.506(5)
O(1)–Cu–O(2)	172.44(12)	172.24(15)	170.18(16)
O(1)–Cu–N(1)	91.93(13)	92.30(18)	92.83(17)
O(1)–Cu–N(3)	91.43(13)	92.28(18)	92.28(16)
O(1)–Cu–O(4)	92.66(12)	88.64(17)	94.10(18)
O(2)–Cu–N(1)	82.11(12)	81.60(17)	81.38(17)
O(2)–Cu–N(3)	93.64(12)	93.35(17)	93.82(16)
O(2)–Cu–O(4)	92.75(11)	96.65(16)	93.56(17)
N(1)–Cu–N(3)	169.37(14)	172.90(2)	174.55(18)
O(4)–Cu–N(1)	97.68(12)	95.23(19)	87.40(2)
O(4)–Cu–N(3)	92.24(12)	90.33(19)	90.40(2)

methanol (in **1**) or perchlorate anion (**2** and **3**) occupies the apical position of the pyramid. The Schiff base ligand coordinates the metal ion in a tridentate fashion forming a five- and a six-membered chelate rings, through the alkoxo oxygen O(1), hydrazinic nitrogen N(1), and the keto oxygen O(2). Inspection of Table 2 indicates that the Cu–O(1), Cu–O(2), and Cu–N(1) bond distances involving the Schiff base are close comparable, being in a range from 1.897(4) to 1.911(3), 1.969(4)–1.977(3), and 1.929(4)–1.940(3) Å, in **1**, **2** and **3**, respectively. These Cu–O and Cu–N bond distances agree with those found in other square pyramidal complexes reported in the literature with similar O,N,O-donor ligands [51].

It is worth to note the Cu–N(py2) of 2.020(4) Å in **1** is sensibly longer than the corresponding values for the 4,4'-bpy in **2** and **3**, of 1.984(5) and 1.965(4) Å, respectively. Since both L¹H and L²H have almost similar structures with identical donor atoms, the difference in the bond lengths may be due to the higher donor strength of 4,4'-bpy than that of pyz, which may also be inferred from their relative pK₁ values of 3.17 and 0.6, respectively [52]. The axial Cu–O bond distance is, as expected, considerably longer than the equatorial ones and show significant differences in length, increasing on going from **1** to **3**, (2.320(3), 2.449(5), 2.506(5) Å).

The distortions in the geometry of the coordination sphere are evident from the deviation of the *cisoid* [81.60(17)–97.68(12)°] and *transoid* measured angles [169.37(14)–174.55(18)°] from the ideal values. The Addison parameter τ [53], defined as $(\beta - \alpha)/60$, where β and α are the two largest coordination angles, provides an index of degree of trigonality, being 0 and 1 for a perfect square pyramidal (SP) geometry and trigonal bipyramidal (TBP), respectively. The calculated value of τ for **1**, **2**, and **3** is 0.05, 0.01 and 0.07, respectively. The metal Cu(II) ion is slightly displaced by 0.13, 0.08 and 0.05 Å from the squared basal plane towards the apical oxygen atom, a feature also evidenced by the coordination angles involving the apical donor, the majority being larger than 90° (Table 2).

In all the complexes the Schiff base atoms are coplanar within ± 0.09 (in **1**), ± 0.26 (**2**), and ± 0.60 Å (**3**), indicating an electron delocalization over this ligand. The dihedral angle formed by N₂O₂ basal coordination plane with the pyz ring in **1** and with the pyridine ring in **2** is of ca. 8°, while the coordinating pyridine in **3** is considerably more tilted (30.9°). The 4,4'-bpy presents a linear conformation in **2** with py rings almost coplanar (4.9°). In **3** the 4,4'-bpy rings are tilted by 10.6° and slightly bowed being the Cu...X...Cu¹ angle (X = centroid of 4,4'-bpy) of 171°.

The phenolic group O(3) in (L¹)[−] (complexes **1** and **2**), which acts as H-bond acceptor for the protonated nitrogen N(2), appears to affect the nuclearity of the complexes and is responsible for the polymeric chains observed in the crystal packing (see below).

Finally the mean basal coordination planes (O(1)/O(2)/N(1)/N(3)) of the symmetry related copper ions in **3** form a dihedral angle of ca. 53.6° (Fig. 3).

3.2. Crystal packing

In complexes **1** and **2**, beside the intra-molecular interaction N(2)–H...O(3), the phenolic group O(3) in turn behaves as H donor to form an intermolecular hydrogen bond O(3)–H...N(4) with the uncoordinated pyz nitrogen of an adjacent unit in **1**, and similarly with pyridine nitrogen N4 in **2**, giving rise to a 1D chain (Figs. 4 and 5). The distances of 2.689(4) and 2.566(6) Å, respectively, indicate a strong O...N interaction. Moreover, the perchlorate anion in **1** is appended to the cationic unit via O(4)–H...O(8) hydrogen bonding interaction involving the coordinated methanol molecule (Fig. 4). Fig. 6 shows a perspective view of the crystal packing down the direction of propagation of the 1D chain in **1**. The relevant hydrogen bonding parameters for all the complexes are listed in Table 3.

Due to the lack of the phenolic group in (L²)[−], complex **3** exhibits inter-molecular hydrogen bonding interaction only, forming a wavy 1D polymeric chain structure (Fig. 7). Here the units are doubly interlocked via N(2)–H...O(5) interactions involving the hydrazinic hydrogen and the oxygen atom O(5) of the coordinated perchlorate of the neighboring unit and vice versa. The N...O distances of 2.849(6) Å indicate a less tight interaction than those measured in **1** and **2**. However the crystal packing is reinforced by π – π interactions occurring between pyridine rings (centroid-to-centroid distance of 3.54 Å) of adjacent chains forming a 2D layered structure parallel to planes (0 1 0).

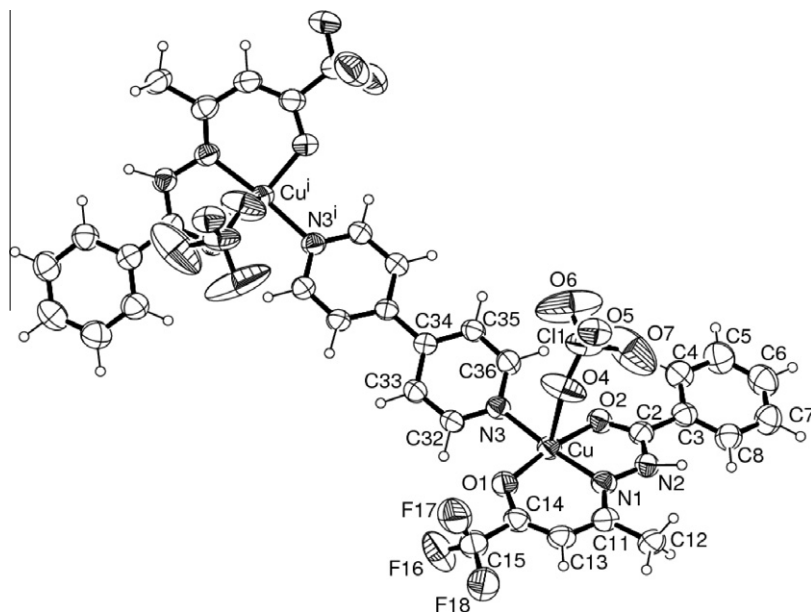


Fig. 3. ORTEP view of **3** located on a crystallographic two-fold axis with atom numbering scheme of the independent unit (thermal displacement ellipsoids are drawn at 40% probability level, $i = x, 1/4 - y, 5/4 - z$).

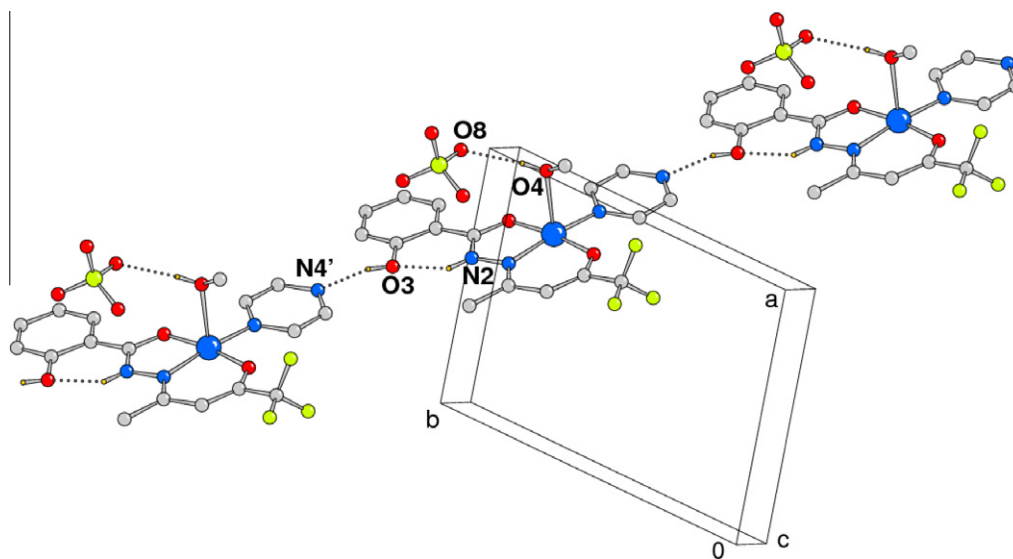


Fig. 4. 1D chain in **1** built up by hydrogen bonds.

In the close comparable mononuclear complexes **1** and **2** the hydrazone ligand L^1H differs from L^2H for the phenolic-OH side arm that appears as structure directing. In fact, as described above, in these species the phenolic group acts as acceptor for intra-ligand hydrogen bonding interaction with the amide hydrogen and at the same time as donor in a strong intermolecular hydrogen bond with the uncoordinated nitrogen atom of pyz and 4,4'-bpy in **1** and **2**, respectively. Possibly, this strong intermolecular interaction hampers the uncoordinated nitrogen atom to form a dinuclear complex, thus propagating the structure in one dimension through hydrogen bonding instead. On the other hand the absence of the phenolic-OH side arm in the ligand L^2H in **3** induces the 4,4'-bpy to act as a bridging species giving rise to a dinuclear complex. However, the formation of one dimensional chain in the solid state of **3** is realized through pairs of weaker intermolecular H-bonds involving the amide N2-H fragment of L^2H and an oxygen atom of the coordinated perchlorate anion of a nearby complex.

3.3. Fourier transform infrared spectra

In the FT-IR spectra of ligands, a strong band assignable to $\nu_{C=N}$ stretching frequency and a strong C=O absorption band are observed around 1640 cm^{-1} and in the region of $1650\text{--}1657\text{ cm}^{-1}$, respectively. Broad N-H absorption bands in the range $3370\text{--}3390$ and $3205\text{--}3220\text{ cm}^{-1}$ are also observed for both ligands. A weak broad band in the region of $3145\text{--}3310\text{ cm}^{-1}$ also indicates the presence of an enolic -OH group in both the ligands, while an additional band at 3040 cm^{-1} is observed for L^1H , due to the phenolic -OH group of benzene ring [54].

Upon complexation the $\nu_{C=N}$ stretching vibration is bathochromically shifted by $25\text{--}35\text{ cm}^{-1}$, and the coordination of azomethine nitrogen is well supported by the peaks at 1615 , 1612 and 1605 cm^{-1} observed for **1**, **2** and **3**, respectively [55,56]. In all the complexes the azomethine coordination is further substantiated by the appearance of a new band in the range $420\text{--}427\text{ cm}^{-1}$

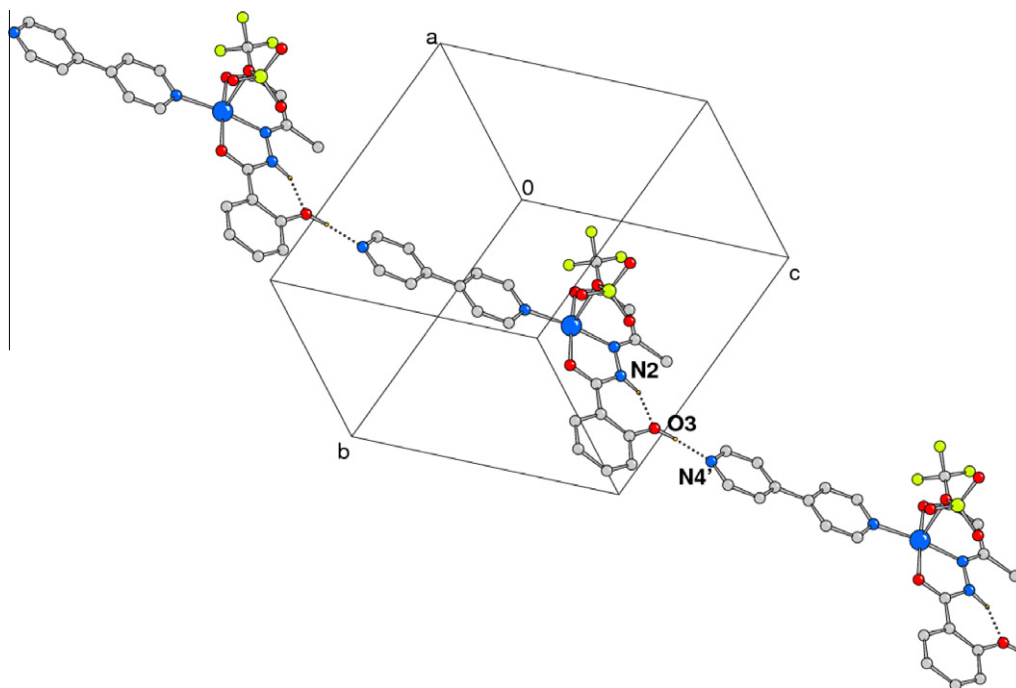


Fig. 5. 1D chain in **2** built up by hydrogen bonds.

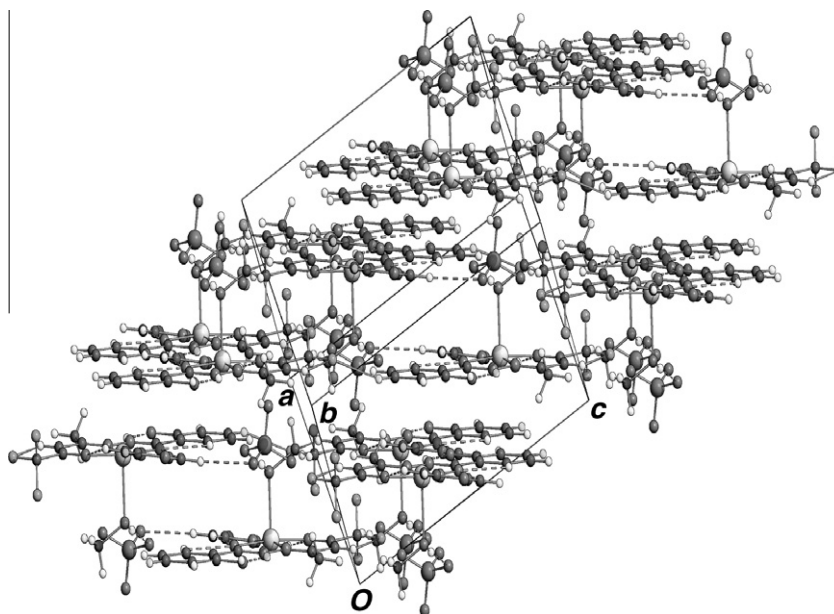


Fig. 6. Crystal packing of **1** viewed down the direction of propagation of polymeric chains.

Table 3
Hydrogen bonding parameters (Å, °) for **1**, **2**, and **3**.

Complex	D–H...A	<i>d</i> (D–H)	<i>d</i> (H...A)	<i>d</i> (D...A)	∠(D–H...A)
1	N(2)–H(1N)...O(3)	0.86	1.91	2.582(4)	133
	O(3)–H(10)...N(4) ^a	0.82	1.90	2.689(4)	162
	O(4)–H...O(8)	0.82	2.01	2.830(5)	175
2	N(2)–H...O(3)	0.96(6)	1.84(6)	2.559(6)	130(5)
	O(3)–H...N(4) ^b	0.91(6)	1.66(6)	2.566(6)	172(7)
3	N(2)–H...O(5) ^c	1.11	1.82	2.849(6)	152

Symmetry codes: ^a1 + *x*, –1 + *y*, *z*; ^b1 + *x*, *y*, –1 + *z*; ^c5/4 – *x*, 1/4 – *y*, *z*.

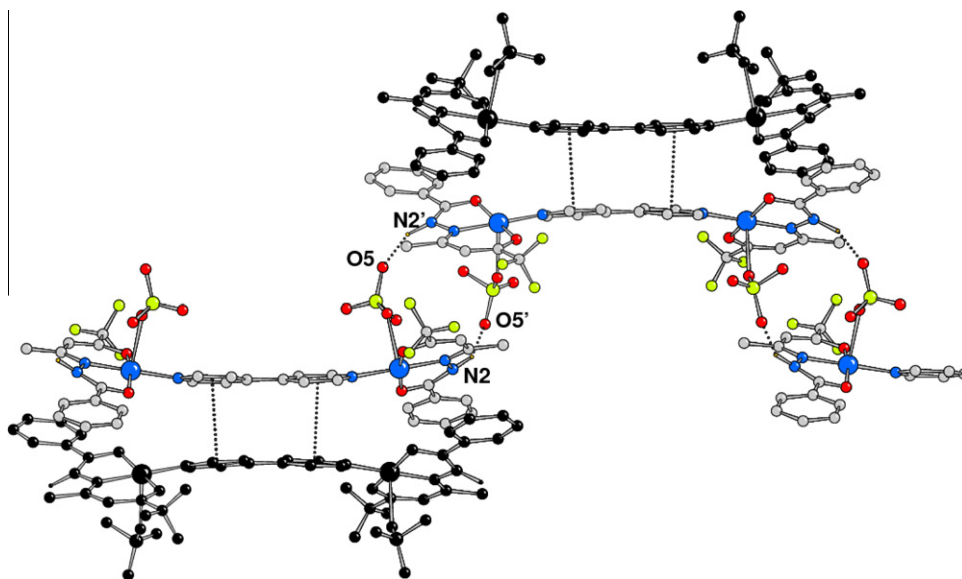


Fig. 7. 1D chain formed by pairs of hydrogen bonds in **3** with indication of π - π interactions between facing pyridine rings of adjacent chains (in black).

assignable to $\nu_{\text{Cu-N}}$ vibration [57]. Moreover a broad band at 3368–3385 cm^{-1} indicates the existence of amide functionality but the broad band in the region of 3145–3310 cm^{-1} assigned to the enolic –OH group is not observed here indicating the deprotonation during complexation. This is further confirmed by the appearance of a new band at 395, 397 and 405 cm^{-1} for **1**, **2**, and **3**, respectively, attributed to $\nu_{\text{Cu-O}}$ stretching. This indicates that the free Schiff base ligands undergo keto-enol tautomerisation in the uncondensed β -keto end during complexation. In the complexes, the band corresponding to $\nu_{\text{C=O}}$ stretching vibration appeared within 1625–1630 cm^{-1} region. Shifting of this band to lower energy region compared to that of the free ligands also indicates the coordination of ketonic oxygen to the metal center. Monodentate coordination mode of pyz in **1** is indicated by the band around 453 cm^{-1} while the bands at 1605, 1411, 1220 and 805 cm^{-1} for **2** and bands at 1540, 1522, 1425, 1225 and 825 cm^{-1} for **3** indicate the monodentate and bridging coordination mode of 4,4'-bpy, respectively [58,59]. In addition, a well resolved peak corresponding to the $\nu_{\text{asym}}(\text{CF}_3)$ vibration appears at 1200 cm^{-1} while a broad trifurcated band in the range 1140–1100 cm^{-1} is also observed in all the spectra assignable to lattice, coordinated perchlorate anions and $\nu_{\text{sym}}(\text{CF}_3)$ vibration [60,61].

3.4. Electronic spectra

Electronic spectra of L^1H and L^2H show a weak band around 370 nm ($\log \epsilon = 3.30$) and another considerably strong band around 255 nm ($\log \epsilon = 3.90$), respectively, assignable to $n \rightarrow \pi^*$ (forbidden) and $\pi \rightarrow \pi^*$ transitions [62,63].

In the spectra of the complexes, the bands of the azomethine chromophore ($n \rightarrow \pi^*$) transition are shifted to lower frequencies indicating that the imine nitrogen atom is involved in coordination to the metal ion. Electronic spectra of **1**, **2**, and **3** show strong absorption bands at 258 ($\log \epsilon = 4.94$), 292 ($\log \epsilon = 4.93$), and 294 nm ($\log \epsilon = 4.92$), respectively, which are clearly charge transfer in origin [64]. The UV absorption bands at 375 ($\log \epsilon = 4.52$), 380 ($\log \epsilon = 4.50$), and 373 nm ($\log \epsilon = 4.60$), observed for **1**, **2** and **3**, respectively, can be correlated to the ligand to Cu(II) charge transfer [LMCT] transition [62]. Complexes **1**, **2** and **3** also exhibit a broad band at 667 ($\log \epsilon = 2.72$), 673 ($\log \epsilon = 2.75$), and 665 nm ($\log \epsilon = 2.81$), respectively. In general typical Cu(II) complexes of

SP or distorted SP geometries exhibit a band in the range 550–660 nm, whereas the corresponding TBP complexes usually show a maximum at $\lambda > 800$ nm with a higher energy shoulder [65,66]. Therefore, these bands inferred the presence of distorted SP geometry of the metal centers in all these complexes which results from ${}^2E \rightarrow {}^2B_1$ transition.

3.5. Electrochemistry

Electrochemical properties of the complexes were revealed by the cyclic voltammograms, recorded in the potential region +1.5 to –1.5 V. On cathodic scan, cyclic voltammograms of **1** and **2** show a single reductive response at the potential –0.42 and –0.37 V (E_{pc}), respectively while **3** shows two reductive responses at –0.44 (E_{pc}^1) and –0.87 V (E_{pc}^2). On anodic scan, the oxidative responses for **1** and **2** appeared at –0.32 and –0.26 V (E_{pa}), respectively and for **3** these appeared at –0.32 (E_{pa}^1) and –0.68 V (E_{pa}^2). Thus peak-to-peak separation ($\Delta E_{\text{p}} = E_{\text{pc}} - E_{\text{pa}}$) for **1** and **2** are 100 and 110 mV while for **3** the peak-to-peak separations are 120 (ΔE_{p}^1) and 190 mV (ΔE_{p}^2). It has been observed for all the complexes that upon increasing the scan rate ΔE_{p} increases, which is always greater than 60 mV and the cathodic peak currents (I_{pc}) are always greater than the anodic peak currents (I_{pa}). These observations indicate the irreversible nature of the redox processes [67]. Controlled potential electrolysis for **1** and **2** carried out at 100 mV more negative to the first reduction wave consumed approximately one electron per molecule ($n \approx 0.93$ for **1** and $n \approx 0.95$ for **2**) indicates that the redox process involves $\text{Cu}^{\text{II}} + e \rightarrow \text{Cu}^{\text{I}}$. Similar controlled potential electrolysis for **3** performed at 100 mV more negative to the first reduction wave consumed approximately one electron ($n \approx 0.91$) and at 100 mV more negative to the second reduction wave consumed approximately two electrons ($n \approx 1.90$) per molecule which indicates the involvement of two electrons corresponds to the process; $\text{Cu}^{\text{II}}\text{Cu}^{\text{II}} \rightarrow \text{Cu}^{\text{II}}\text{Cu}^{\text{I}} \rightarrow \text{Cu}^{\text{I}}\text{Cu}^{\text{I}}$. The redox behaviors of the complexes are very similar to some of the previously reported mono- and binuclear complexes in the literature [58,68,69].

3.6. Magnetic properties

The magnetic properties of **1**, **2** and **3** were evaluated by means of bulk magnetization measurements. The value of the product of

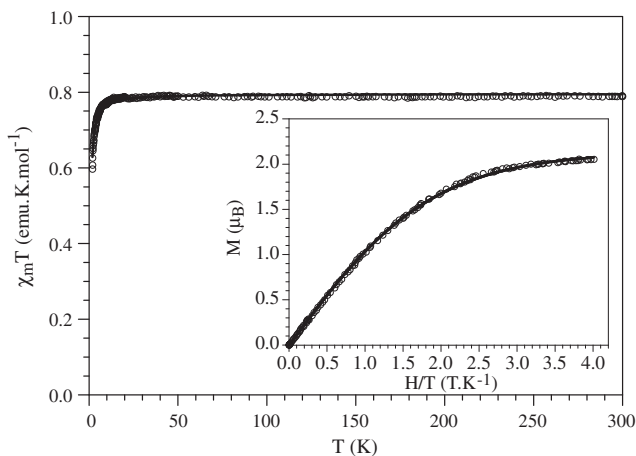


Fig. 8. Thermal variation of the $\chi_m T$ product per Cu(II) dimer in compound **3**. Inset shows the isothermal magnetization at 2 K. Solid lines represent the best fit to the models (see text).

the molar magnetic susceptibility times the temperature, $\chi_m T$ at 300 K ($0.428 \text{ emu K mol}^{-1}$) for the powdered samples of **1** and **2** are close to the spin-only value expected for a $S = \frac{1}{2} d^9$ Cu(II) compound with $g = 2.15$.

The thermal variation of $\chi_m T$ product for compound **3** shows at room temperature a value of ca. $0.80 \text{ emu K mol}^{-1}$ (Fig. 8), which is close to that expected for two noninteracting Cu(II), $S = 1/2$ ions ($0.75 \text{ emu K mol}^{-1}$ for $g = 2.0$). When cooling down the sample, the $\chi_m T$ product remains constant down to ca. 10 K and below this temperature $\chi_m T$ shows a smooth progressive decrease to reach a minimum value of ca. $0.60 \text{ emu K mol}^{-1}$ at 2 K (Fig. 8). This behavior for **3** indicates a very weak antiferromagnetic coupling, responsible of the decrease observed at low temperature. According to the dimeric structure of this compound, we have fit the magnetic data with the Bleaney and Bowers expression for a simple $S = 1/2$ dimer (the Hamiltonian is written as $H = -JS_{i+1}$) [70]. This model reproduces very satisfactorily the magnetic data of **3** in the whole temperature range with $g = 2.0596(5)$ and $J = -1.38(1) \text{ K} = -0.96(1) \text{ cm}^{-1}$ (solid line in Fig. 8).

A further confirmation of the weak antiferromagnetic coupling comes from the isothermal magnetization at 2 K that shows a saturation value close to $2 \mu_B$ (as expected for two noninteracting $S = 1/2$ copper(II) ions with $g = 2$) (inset in Fig. 8) and by the fact that the isothermal magnetization can be very well reproduced with a Brillouin function for two $S = 1/2$ ions with a g value of $2.134(3)$ with a weak interaction of $-0.71(1) \text{ K} = -0.49(1) \text{ cm}^{-1}$, solid line in the inset in Fig. 8.

The very weak antiferromagnetic coupling observed in complex **3** is in agreement with the expected behavior for a dinuclear copper(II) complex where the metals are separated by more than 10 \AA through the long 4,4'-bpy bridge [71–73].

4. Conclusion

The present study describes the synthesis, spectral, structural and magnetic characterization of three new Cu(II) complexes with two Schiff base hydrazones. The X-ray structural analyses identify the unusual monodentate coordination of pyrazine and 4,4'-bipyridine in two cases (complexes **1** and **2**) and reveal that the phenolic –OH side arm in the Schiff base ligand plays a dominant role to address the complexes towards mononuclear species and the formation of polymeric chains achieved through hydrogen bonding interactions. Magnetic measurements reveal the presence of very weak antiferromagnetic exchange interactions in the dinuclear

complex **3** that can be well reproduced with a simple $S = 1/2$ dimer model with $J = -1.38(1) \text{ K} = -0.96(1) \text{ cm}^{-1}$, in agreement with the expected behavior for a dinuclear copper(II) complex with metals separated by more than 10 \AA through the long 4,4'-bipyridine spacer.

Acknowledgments

S.S. gratefully acknowledges Dr. J. Chakraborty, DRDO, Kanpur, India for his valuable suggestions. S.K.D. and S.M. acknowledge University Grants Commission, New Delhi, India for financial assistance. We also acknowledge the European Union (MAGMANet network of excellence), the Spanish Ministerio de Educación y Ciencia (Projects MAT2007-61584 and CSD 2007-00010 Consolider-Ingenio in Molecular Nanoscience) and the Generalitat Valenciana (Project PROMETEO/2009/095) for funding this research work.

Appendix A. Supplementary material

CCDC 671674, 671675, and 671676 contain the supplementary crystallographic data for **1**, **2**, and **3**. These data can be obtained free of charge from The Cambridge Crystallographic Data Centre via www.ccdc.cam.ac.uk/data_request/cif. Supplementary data associated with this article can be found, in the online version, at doi:10.1016/j.ica.2011.01.008.

References

- [1] B. Xiao, H. Hou, Y. Fan, M. Tang, *Inorg. Chim. Acta* 360 (2007) 3019 (and references therein).
- [2] D. Bose, J. Banerjee, S.H. Rahaman, G. Mostafa, H.-K. Fun, R.D.B. Walsh, J. Zaworotko, B.K. Ghosh, *Polyhedron* 23 (2004) 2045.
- [3] S. Rollas, S.G. Küçükgül, *Molecules* 12 (2007) 1910.
- [4] S. Abram, C. Maichle-Mössner, U. Abram, *Polyhedron* 17 (1998) 131.
- [5] G.F. de Sousa, C.A.L. Filgueiras, A. Abras, S.S. Al-Juaid, P.B. Hitchcock, J.F. Nixon, *Inorg. Chim. Acta* 218 (1994) 139.
- [6] D. Wester, G.J. Palenik, *Inorg. Chem.* 15 (1976) 755.
- [7] K. Andjelković, I. Ivanović, S.R. Niketić, B. Prelesnik, V.M. Leovac, *Polyhedron* 16 (1997) 4221.
- [8] K. Andjelković, G. Jakovljević, M. Zlatović, Ž. Tešić, D. Sladić, J. Howing, R. Tellgren, *J. Serb. Chem. Soc.* 69 (2004) 651.
- [9] A. Bonardi, C. Merlo, C. Pelizzi, G. Pelizzi, P. Tarasconi, F. Vitali, F. Cavatorta, *J. Chem. Soc., Dalton Trans.* (1991) 1063.
- [10] G.J. Palenik, D.W. Wester, *Inorg. Chem.* 17 (1978) 864.
- [11] S. Rao, D.D. Mishra, R.V. Mourya, N. Nageswara, *Polyhedron* 16 (1999) 1825.
- [12] E. Fujita, B.S. Brunschwig, T. Ogata, S. Yanagida, *Coord. Chem. Rev.* 132 (1994) 195.
- [13] E. Kimura, S. Wada, M. Shionoya, Y. Okazaki, *Inorg. Chem.* 33 (1994) 770.
- [14] D.X. West, A.E. Liberta, S.B. Padhye, R.C. Chikate, P.B. Sonawane, A.S. Kumbhar, R.G. Yerande, *Coord. Chem. Rev.* 123 (1993) 49.
- [15] S.K. Sridhar, M. Saravanan, A. Ramesh, *Eur. J. Med. Chem.* 36 (2001) 615.
- [16] B. Bottari, R. Maccari, F. Monforte, R. Ottana, E. Rotondo, M. Vigorita, *Bioorg. Med. Chem. Lett.* 10 (2000) 657.
- [17] B. Kaymakciogul, S. Rollas, *Il Farmaco* 57 (2002) 595.
- [18] E. Ainscough, A. Brodie, J. Ranford, M. Waters, *Inorg. Chim. Acta* 236 (1995) 83.
- [19] E. Ainscough, A. Brodie, J. Ranford, M. Waters, *Inorg. Chim. Acta* 267 (1998) 27.
- [20] J. Easmon, G. Puerstinger, T. Roth, H. Feibig, M. Jenny, W. Jaeger, G. Heinisch, J. Hofmann, *Int. J. Cancer* 94 (2001) 89.
- [21] S. Küçükgül, S. Rollas, I. Küçükgül, M. Kiraz, *Eur. J. Med. Chem.* 34 (1999) 1093.
- [22] L.-M. Wu, H.-B. Teng, X.-B. Ke, W.-J. Xu, J.-T. Su, S.-C. Liang, X.-M. Hu, *Chem. Diversity* 4 (2007) 2198.
- [23] S. Gupta, S. Pal, A.K. Barik, A. Hazra, S. Roy, T.N. Mandal, S.-M. Peng, G.-H. Lee, M.S. El Fallah, J. Tercero, S.K. Kar, *Polyhedron* 27 (2008) 2519.
- [24] N.M.H. Salem, L. El-Sayed, M.F. Iskander, *Polyhedron* 27 (2008) 3215.
- [25] Z. Xu, L.K. Thompson, D.O. Miller, *Polyhedron* 21 (2002) 1715.
- [26] M.F. Iskander, T.E. Khalil, R. Werner, W. Haase, I. Svoboda, H. Fuess, *Polyhedron* 19 (2000) 949.
- [27] G.-C. Xu, L. Zhang, L. Liu, G.-F. Liu, D.-Z. Jia, *Polyhedron* 27 (2008) 12.
- [28] P.B. Sreeja, M.R.P. Kurup, A. Kishore, C. Jasmin, *Polyhedron* 23 (2004) 575.
- [29] M.F. Iskander, L. El-Sayed, N.M.H. Salem, W. Haase, H.J. Linder, S. Foro, *Polyhedron* 23 (2004) 23.
- [30] M.F. Iskander, T.E. Khalil, R. Werner, W. Haase, I. Svoboda, H. Fuess, *Polyhedron* 19 (2000) 1181.
- [31] F. Hueso-Ureña, A.L. Peñas-Chamorro, M.N. Moreno-Carretero, J.M. Amigó, V. Esteve, T. Debaerdemaeker, *Polyhedron* 18 (1999) 2205.

- [32] S.K. Dey, B. Bag, Z. Zhou, A.S.C. Chan, S. Mitra, *Inorg. Chim. Acta* 357 (2004) 1991 (and references therein).
- [33] J.-M. Lehn, *Proc. Natl. Acad. Sci. USA* 99 (2002) 4763.
- [34] C.B. Aakeröy, A.M. Beatty, *Aust. J. Chem.* 54 (2001) 409.
- [35] A.N. Khlobystov, A.J. Blake, N.R. Champness, D.A. Lemenovskii, A.G. Majouga, N.V. Zyk, M. Schröder, *Coord. Chem. Rev.* 222 (2001) 155.
- [36] SMART: Bruker's CCD Data Collection Program, Madison, Wisconsin, USA.
- [37] Enraf-Nonius COLLECT, Nonius BV, Delft (The Netherlands), 1997–2000.
- [38] SAINT v4: Software Reference Manual, Siemens Analytical X-ray Systems, Madison, WI, USA, 1996.
- [39] Nonius COLLECT, DENZO, SCALEPACK, SORTAV: KappaCCD Program US B.V., Delft, The Netherlands, 1999.
- [40] SIR92 – a program for automatic solution of crystal structures by direct methods: A. Altomare, G. Cascarano, C. Giacovazzo, A. Guagliardi, M.C. Burla, G. Polidori, M. Camalli, *J. Appl. Crystallogr.* 27 (1994) 435.
- [41] SIR97 – a new tool for crystal structure determination and refinement: A. Altomare, M.C. Burla, M. Camalli, G.L. Cascarano, C. Giacovazzo, A. Guagliardi, A.G.G. Moliterni, G. Polidori, R. Spagna, *J. Appl. Crystallogr.* 32 (1999) 115.
- [42] G.M. Sheldrick, *Acta Crystallogr., Sect. A* 64 (2008) 112.
- [43] L.J. Farrugia, *J. Appl. Crystallogr.* 30 (1997) 565.
- [44] L.J. Farrugia, *J. Appl. Crystallogr.* 32 (1999) 837.
- [45] J.S. Haynes, S.J. Rettig, J.R. Sams, J. Trotter, R.C. Thompson, *Inorg. Chem.* 27 (1988) 1237.
- [46] S.-Y. Yang, L.-S. Long, R.-B. Huang, L.-S. Zheng, S.W. Ng, *Acta Crystallogr., Sect. E* 59 (2003) m841.
- [47] T. Otieno, A.M. Gipson, S. Parkin, *J. Chem. Crystallogr.* 32 (2002) 81.
- [48] L.A. Glinskaya, R.F. Klevtsova, T.E. Kokina, S.V. Larionov, *J. Struct. Chem.* 42 (2001) 982.
- [49] R. Karmakar, C.R. Choudhury, S. Mitra, L. Dahlenburg, *Struct. Chem.* 16 (2005) 611.
- [50] K. Abu-Shandi, C. Janiak, B. Kersting, *Acta Crystallogr., Sect. C* 57 (2001) 1261.
- [51] D. Plaul, A. Buchholz, H. Görls, W. Plass, *Polyhedron* 26 (2007) 4581.
- [52] R.D. Bailey, G.W. Drake, M. Grabarczyk, T.W. Hanks, L.L. Hook, W.T. Pennington, *J. Chem. Soc., Perkin Trans. 2* (1997) 2773 (and references therein).
- [53] A.W. Addison, T.N. Rao, J. Reedijk, J. van Rijn, G.C. Verschoor, *J. Chem. Soc., Dalton Trans.* (1984) 1349.
- [54] N. Mondal, D.K. Dey, S. Mitra, K.M. Abdul Malik, *Polyhedron* 19 (2000) 2707.
- [55] P. Bindu, M.R.P. Kurup, T.R. Satyakeerthy, *Polyhedron* 18 (1999) 321.
- [56] P. Bindu, M.R.P. Kurup, *Transition Met. Chem.* 22 (1997) 578.
- [57] E.B. Sena, M.R.P. Kurup, *Polyhedron* 26 (2007) 829.
- [58] S. Banerjee, S. Mondal, S. Sen, S. Das, D.L. Hughes, C. Rizzoli, C. Desplanches, C. Mandal, S. Mitra, *Dalton Trans.* (2009) 6849 (and references therein).
- [59] L.-P. Zhang, L.-G. Zhu, *Cryst. Eng. Commun.* 8 (2006) 815.
- [60] K. Nakamoto, *Infrared and Raman Spectra of Inorganic and Coordination Compounds, Part A and B, fifth ed.*, John Wiley, New York, 1997.
- [61] R.T. Conley, *Infrared Spectroscopy*, Allyn and Bacon, Boston, 1966.
- [62] A. Golcu, M. Tumer, H. Demirelli, R.A. Wheatley, *Inorg. Chim. Acta* 358 (2005) 1785.
- [63] S. Banerjee, A. Ray, S. Sen, S. Mitra, D.L. Hughes, R.J. Butcher, S.R. Batten, D.R. Turner, *Inorg. Chim. Acta* 361 (2008) 2692.
- [64] A.B.P. Lever, *Inorganic Electronic Spectroscopy*, second ed., Elsevier, Amsterdam, 1984.
- [65] U. Mukhopadhyay, I. Bernal, S.S. Massoud, F.A. Mautner, *Inorg. Chim. Acta* 357 (2004) 3673.
- [66] Y. Song, D.-R. Zhu, K.-L. Zhang, Y. Xu, C.-Y. Duan, X.-Z. You, *Polyhedron* 19 (2000) 1461.
- [67] N. Sengottuvelan, J. Manonmani, M. Kandaswamy, *Polyhedron* 21 (2002) 2767.
- [68] S. Sreedaran, K.S. Bharathi, A.K. Rahiman, L. Jagadish, V. Kaviyaran, V. Narayanan, *Polyhedron* 27 (2008) 2931.
- [69] T.M. Rajendiran, R. Venkatesan, P.S. Rao, M. Kandaswamy, *Polyhedron* 17 (1998) 3427.
- [70] B. Bleaney, K.D. Bowers, *Proc. R. Soc. London Ser. A* 214 (1952) 451.
- [71] A.-R. Song, Y. Song, X.-M. Ouyang, Y.-Z. Li, W.-Y. Sun, *Inorg. Chem. Commun.* 8 (2005) 186.
- [72] S. Benmansour, F. Setifi, C.J. Gómez-García, S. Triki, E. Coronado, *Inorg. Chim. Acta* 361 (2008) 3856.
- [73] H. Liu, C.J. Gómez-García, J. Peng, J. Sha, L. Wang, Y. Yan, *Inorg. Chim. Acta* 362 (2009) 1957.